

Permittivity of geotextiles with biaxial tensile loads

Edwards, M. and Hsuan, G.

Department of Civil, Architectural and Environmental Engineering, Drexel University, Philadelphia, PA, USA

Keywords: geotextile, filtration, tensile load

ABSTRACT: This study evaluated the permittivity of geotextiles, in terms of flow rate, while being subjected to biaxial tensile stresses. Seven types of geotextiles were used and they included needle-punched and heat-set nonwoven, slit-film, polyester and polypropylene woven geotextiles. A cross-shaped test specimen was used. The applied longitudinal tensile stresses ranged from 10% to 60% of the ultimate tensile strength, where the transverse tensile stress was kept at a ratio of 1:4 with respect to the applied longitudinal stress. The permittivity was measured under a constant hydraulic head of 25 mm. The permittivity test results of the biaxially loaded geotextiles were compared with those obtained from the uniaxially loaded geotextiles. For the two nonwoven geotextiles and slit-film woven geotextile, the changes of flow rates in the biaxially loaded condition behave similarly to the uniaxially loaded condition. However, for more complex weaved woven geotextiles, the effect of biaxial tensile loads on the flow rate is opposite to that with uniaxial loads.

1 INTRODUCTION

Filtration is one of the most common functions of geotextiles. It involves liquid flow across the plane of the geotextile, while retaining the solid on its upstream side. In most geotechnical applications, the geotextile is subjected to a compressive load due to the soil above, while water is being filtered. The current two standard methods for determining permittivity of geotextiles are ASTM D 4491 and ASTM D 5493. ASTM D 4491 specifies permittivity of geotextiles in an uncompressed state, while, ASTM D 5493 presents the test method for geotextiles subjected to normal compressive loads. None of these two tests, however, consider axial tensile stresses in the geotextiles, as experienced in geotextiles used for filtration in geotextile tube applications. In the instance of dewatering, a circumferential tensile stress is generated in the geotextile tube during the filling stage. Such stress can have an effect on the water flow rate by changing the opening size of the geotextile. The dewatering behavior can vary significantly due to different orientation of the geotextile with respect to the axial direction of the geotextile tube, as described by Gaffney et al. (2009). Further, Fourie and Kuchena (1995) noted that there is a reduction in both initial and equilibrium flow rates

with increasing uniaxial tensile loads, when considering soil-geotextile systems.

In this paper, the flow behavior of the geotextile while subject to biaxial tensile loading was evaluated. Seven different geotextiles were tested; they included two types of nonwoven geotextiles and five types of woven geotextiles. Loads of up to 60% of the tensile strength of the geotextile were applied in the majority of the tests.

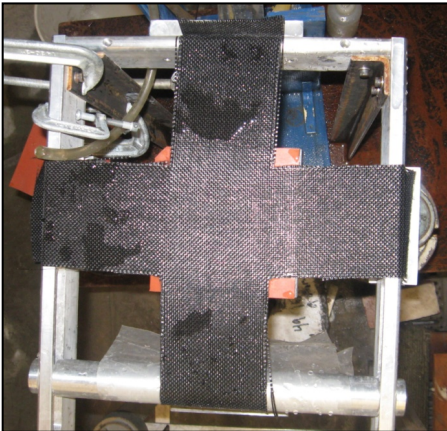
2 TEST DESCRIPTION

2.1 Test apparatus

The test apparatus, shown in Figures 1a and 1b, was designed for testing geotextiles under uniaxial and biaxial tensile loads of up to 0.0263 kN/mm applied over a 100 mm. The device incorporated a loading system whereby the geotextile can be subjected to uniaxial or biaxial tensile loading, while measuring the flow rate.

The loading frame consisted of a moveable rod across its width to accommodate geotextile samples of lengths 500 to 760 mm (Figure 1b). A constant head permittivity device was positioned between the end of the test frame and the moveable rod. The permittivity device was separated into upper and lower units. A rubber membrane, 2 mm in thickness, was attached to the surface of upper and lower units to minimize the transmissivity flow along the

geotextile during the test. The upper unit maintained a constant head, while the desired hydraulic head was introduced by rotating the discharge pipe that was connected to the lower unit. The hydraulic head was monitored by two piezometers that were connected to the upper and lower units. The flow area was a 50 mm diameter circle. Water was supplied from a reservoir that was refilled directly with tap water. Once filled, the reservoir tank was left overnight in order to minimize air bubbles generated during the test.



a) Plan view of specimen



b) Loaded specimen

Figure 1: Permittivity test apparatus

2.2 Test procedure

A cross-shaped specimen, 760 mm long (longitudinal side) by 760 mm wide (transverse side), was used in this test (Figure 1a). An internal width of the specimen was 100 mm was chosen due to the loading capacity of the frame. Also, to be consistent, the ultimate tensile strength was evaluated using 100 mm wide specimens instead of 200 mm wide as defined

in ASTM D4885. The test specimens were fully saturated with water prior to the test. One end of the longitudinal portion of the specimen was secured to the end of the test frame, while the transverse sides were laid over the sides of the loading frame. The other longitudinal end of the specimen was passed over the lower unit of the permittivity device and laid over the moveable rod. The three free ends of the specimen were clamped with the serrated grips, to which a loading platforms were attached (Figure 1b). The load applied on each transverse side was 1/4 of that applied in the longitudinal direction. The moveable rod was locked into a position, so that sufficient clearance between the loading platform and the floor was assured. The upper permittivity unit was placed on top of the specimen and aligned with the lower unit. Four C-clamps were used to secure the upper and lower units. Water was backfilled through the discharge pipe, up to the top of the lower unit, such that the water level was in contact with geotextile specimen. Bubbles that formed in the pipe were eliminated through the bleed valve.

At each loading, the upper permittivity unit was removed and the desired weight was applied. In order to mobilize the axial tensile stress, the specimen was left with the suspended weight for fifteen (15) minutes during which the specimen was fully saturated with water provided from the lower unit. After that duration, the upper unit was re-secured and water was again backfilled through the discharge pipe.

3 TEST MATERIALS

Seven types of geotextiles were tested. They were needle-punched nonwoven (NW), heat-set nonwoven (NW), slit-film woven (SF-woven), weft insertion knitted, polyester woven (WIK-PET-woven), and three different types of polypropylene woven geotextiles (PP-woven-2, PP-woven-3 and PP-woven-4).

One specimen was cut for each of the nonwoven geotextiles, and the three polypropylene woven geotextiles, with the cross-machine direction (XMD) along the longitudinal for the latter. Two samples were cut for each of the SF-woven and WIK-PET-woven geotextiles, one in the machine and the other in the cross-machine direction, along the longitudinal.

It was assumed that the tensile strengths of the nonwoven geotextiles were the same in both directions. Two replicates were tested for each geotextile, with the exception of the three PP woven geotextiles due to limited availability of the materials.

Table 1 Properties of tested geotextiles.

| Sample | Flow Rate ⁽¹⁾ (l/sec/m ²) | Ultimate Tensile Strength, (kN/m) | |
|-----------------------------|---|-----------------------------------|----------------------|
| | | MD | XMD |
| Needle-punched NW | 74.4 | 13.1 ⁽²⁾ | - |
| Heat-set NW | 7.1 | 8.4 ⁽²⁾ | - |
| SF-woven | 7.4 | 33.3 ⁽²⁾ | 44.8 ⁽²⁾ |
| Weft Insertion Knitted, PET | 87.6 | 121.8 ⁽³⁾ | 111.1 ⁽³⁾ |
| PP-woven-2 | 13.5 | 79.6 ⁽³⁾ | 80.5 ⁽³⁾ |
| PP-woven-3 | 10.0 | 78.2 ⁽³⁾ | 80.5 ⁽³⁾ |
| PP-woven-4 | 10.7 | 58.3 ⁽³⁾ | 58.3 ⁽³⁾ |

- ⁽¹⁾ ASTM D 4491 (50-mm hydraulic head)
⁽²⁾ Measured by ASTM D 4885 (using 100 mm wide specimen)
⁽³⁾ Manufacturer's data (using 200 mm wide specimen)

4 RESULTS

4.1 Permittivity with biaxial loads

4.1.1 Nonwoven geotextiles

Figure 2 and Figure 3 show graphs of the flow rate retained versus applied tensile load along the longitudinal for the needle-punched NW and heat-set NW geotextiles, respectively. (Note that the test specimen was subjected to the transverse loading equal to the quarter of the longitudinal load).

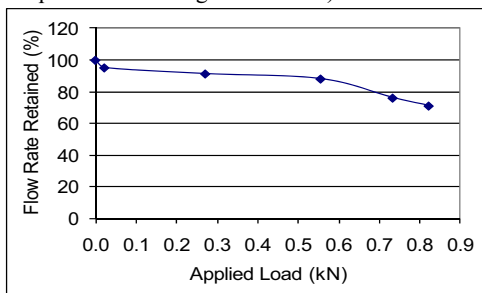


Figure 2. Flow rate retained versus applied load of the needle-punched NW geotextile.

The needle-punched NW geotextile sample shows a slight initial decrease in the flow rate retained, after which it is relatively steady up to an applied load of 0.556 kN, followed by a gradual decrease. The flow rate retained decreases by 39 % when the tensile load increases from 0 to 0.823 kN (62% of the ultimate tensile strength).

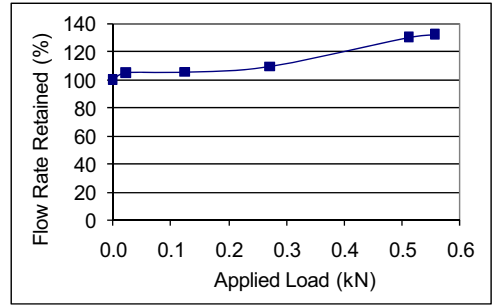


Figure 3. Flow rate retained versus applied load of the heat-set NW geotextile

In contrast, the heat-set NW (Figure 3) exhibits the opposite behavior, whereby there is a small increase in flow rate retained, then increases slowly up to an applied longitudinal tensile load of 0.271 kN, after which a sharp increase by 32% when loaded to 0.556 kN (65% of the ultimate tensile strength).

The decrease in the flow rate retained for the needle-punched NW can be attributed to the necking along the longitudinal direction of the specimen as the load increased during the test, thus reducing the void sizes of the geotextile. The heat-set NW geotextile did not experience the necking phenomenon owing to the thermal bonding. The increase in the flow rate retained is likely caused by the breaking of the thermal bonding as axial loading increased, resulting in the opening up the voids.

4.1.2 Woven geotextiles

Figures 4 through 6 show graphs of the flow rate retained versus applied longitudinal tensile load for the woven geotextile samples.

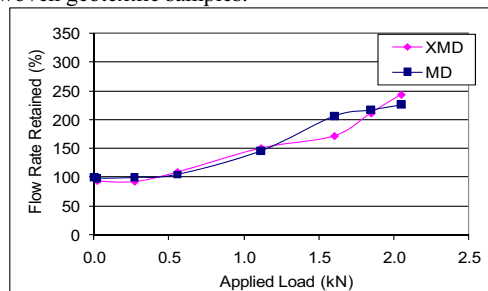


Figure 4. Flow rate retained versus applied load of the SF-woven geotextile.

The slit-film geotextile sample exhibits similar profiles in the MD and XMD; the flow rate retained increases steadily with increasing longitudinal tensile load. Although the tensile strengths of the MD and XMD of the geotextile are not the same, the flow rate retained increases by about 135 % at the applied load of 2.046 kN in both cases (Figure 4).

Similar changes in flow rate are also exhibited in the WIK-PET-woven geotextile samples whereby the flow rate retained profiles with applied longitudinal tensile load have an increasing trend in both orientations. The flow rate retained values increase by approximately 43% at an applied load 2.046 kN in both cases (Figure 5).

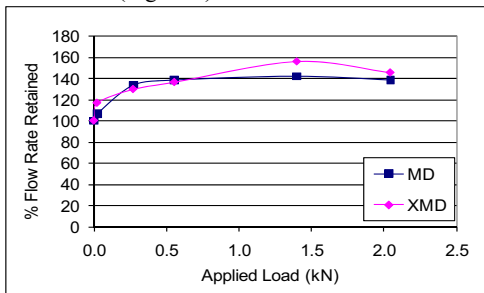


Figure 5. Flow rate retained versus applied load of the WIK-PET-woven geotextile.

Figure 6 shows the effect of biaxial loading on the flow rate retained of the three PP woven geotextile samples in the XMD. For the PP-woven-2 geotextile, the flow rate retained decreases by 47 % at 1.179 kN of applied longitudinal load, after which, the flow rate retained is essentially unchanged, even though the load increases to 2.113 kN.

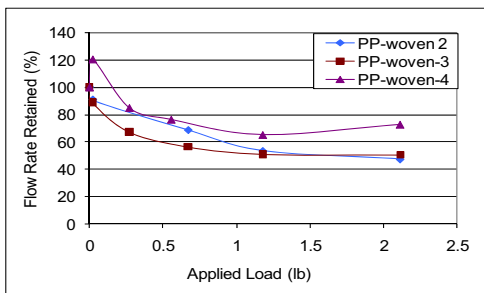


Figure 6. Flow rate retained versus applied load of the three polypropylene woven geotextiles.

For the PP-woven-3-woven geotextile, the flow rate retained decreases steadily and reaches an asymptote at 50%, when loaded from 0 to 2.113 kN.

The flow through the XMD specimen of the PP-woven-4-woven geotextile exhibits an initial increase in flow rate retained and decreases by about 27% when loaded to 2.113 kN. The maximum reduction in flow rate retained of 35% is experienced at an applied load of 1.179 kN (20% of the UTS).

5 DISCUSSION

The two nonwoven geotextiles exhibit contrasting behavior while subjecting to biaxial tensile loading. The needle-punched NW geotextile shows a de-

crease in flow rate retained whereas, the heat-set NW geotextile experiences an increase (Figures 2 and 3). These two trends are similar to the trends obtained in the previous study (Figure 7), in which the geotextiles were loaded uniaxially (Edwards et al 2009).

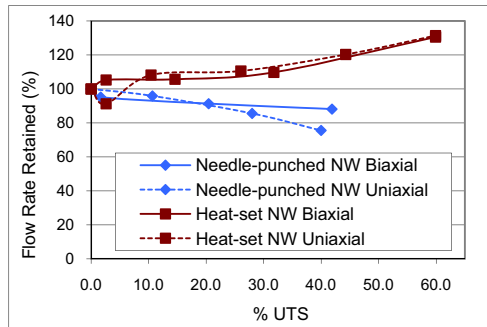


Figure 7. Flow rate retained versus % UTS of Needle-punched and Heat-set NW geotextiles.

The amount of decrease in flow rate retained for the needle-punched NW geotextile, when loaded biaxially, decreases 22% less than that under uniaxial loads, at an applied load of about 40 % ultimate tensile strength (UTS). This difference can be attributed to the effect of the confining transverse loads which reduce, but does not eliminate, necking. On the other hand, biaxial loading only has a slight effect on the flow rate in comparison to the uniaxially loaded, for the heat-set NW geotextile. The breaking of thermal bonds, as the uniaxial loads are applied, is likely the reason for the increase and the additional transverse loads do not have a large effect on the flow rate behavior.

In the case of the woven geotextiles, the flow rate retained increases for the SF-woven and WIK-PET-woven geotextiles, while the flow rate retained decreases for the three PP woven geotextiles in the XMD. Both the SF-woven and the WIK-PET-woven geotextiles behave similarly, insofar as, they experience comparable amounts of increases in flow rate retained in the cross-machine and machine directions.

The SF-woven geotextile has a comparable magnitude of increase to that of a uniaxially loaded specimen at the load of 1.846 kN. The percent increase in flow rate retained in the uniaxial case is 100 % versus 114 % in the biaxially loaded case. The transverse loads do not contribute to additional changes in the flow behavior of the geotextile than when subjected to uniaxial loads.

Figure 8, (flow rate retained against the applied longitudinal load expressed as a percentage of the UTS of the WIK-PET-woven geotextile), illustrates that the biaxially loaded WIK-PET-woven geotextile behaves differently in the MD direction than when

loaded uniaxially. In the latter case, the MD specimen experiences a 10 % decrease in flow rate retained. The additional transverse loads lead to an increase of 40% in the flow rate retained. The transverse loads limit the deformation of the geotextile under uniaxial loading that lead to the expanding of voids. However, there is no significant difference in the flow behavior of the XMD between two different loading conditions.

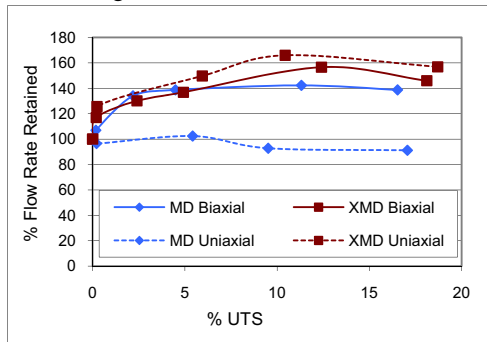


Figure 8. Flow rate retained versus % UTS of WIKPET-woven geotextile.

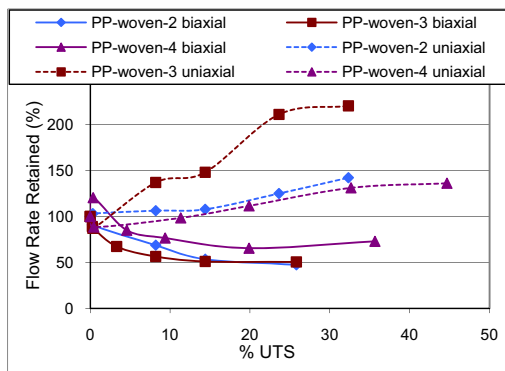


Figure 9. Flow rate retained versus % UTS of the three PP-woven geotextiles.

Figure 9 shows the flow rate retained against the applied longitudinal load expressed as a percentage of the UTS of PP-woven-2, PP-woven-3, and PP-woven-4 geotextile specimens in the XMD. All specimens, regardless of the type of geotextile, behave similarly under biaxial tensile loading; their flow rates are approaching an asymptote. The behavior in the uniaxial case is the complete opposite, where an increase with applied load is experienced for each specimen.

In the biaxial case, the PP-woven-2 and PP-woven-3 geotextiles show similar flow behavior with increasing biaxial tensile load. Further, both geotextiles have the same ultimate tensile strengths in the XMD and experienced comparable magni-

tudes of decrease in flow rate retained, 47% and 50% respectively.

The curve of flow rate retained (biaxial loading) for PP-woven-4 follows the same trend as the PP-woven-2 and PP-woven-3 but shows a lower magnitude of decrease. This may be due to the lower tensile strength of the PP-woven-4 geotextile, as compared to the other two, and thus achieving the limit of deformation at a faster rate.

It is interesting to note that this decreasing trend is in contrast to the behavior when uniaxial tensile loads were applied. Actually, for all three specimens, the flow rate increases with the uniaxial load in the XMD (Edwards et al. 2009). The flow rate retained of the PP-woven-3 specimen increases almost three times as much as the PP-woven-2 (Figure 9). Also, the flow rate retained curve of the PP-woven-2 geotextile behaves more like the PP-woven-4 geotextile when loaded uniaxially.

Table 2. Filtration comparison.

| Paper | Condition | Test | Behavior |
|--------------------------------|------------------------|--------------|----------------------|
| <u>Needle Punched Nonwoven</u> | | | |
| Fourie & Addis 1997 | Biaxial (L/T = 1) | FOS | Decrease |
| | Biaxial (Variable L/T) | | Increase |
| | Biaxial (L/T = 1) | Permeability | Increase |
| Edwards et al. | Biaxial (L/T = 4) | Permeability | Decrease |
| <u>Silt-Film Woven</u> | | | |
| Fourie & Addis 1997 | Biaxial (L/T = 1) | FOS | Decrease |
| | Biaxial (Variable L/T) | | Decrease |
| | Biaxial (L/T = 1) | Permeability | Decrease |
| Fourie & Addis 1999 | Biaxial (L/T = 1) | FOS | Decrease or Increase |
| | Biaxial (Variable L/T) | | Decrease |
| Edwards et al. | Biaxial (L/T = 4) | Permeability | Increase |

The effect of biaxial tensile loads on the filtration characteristics of geotextiles have been studied by Fourie and Addis (1997 and 1999). They conducted hydrodynamic sieving and falling head permeability tests on SF-woven geotextiles and a needle-punched NW geotextile under biaxial tensile loadings. The hydrodynamic sieving test was used to

evaluate the filtration opening size (FOS), defined as 95% (by mass) of the diameter of the glass beads that have passed through the geotextile during the sieving process.

Table 2 shows a comparison between the results of Fourie and Addis and this study. Fourie and Addis applied biaxial loads in two ways: firstly, where the longitudinal (L) and transverse loads (T) were equal ($L/T = 1$) and secondly, where the longitudinal and transverse loads were unequal, resulting in a variable L/T ratio. In this study, biaxial loads were applied with a fixed L/T ratio of 4.

Considering the needle-punched NW geotextile, there is a decreasing trend of the FOS with applied biaxial load at a constant L/T ratio, but an increasing trend when L/T was variable. The permeability increased, though, with the application of equal biaxial loads. This contradicts the permeability behavior found in this study.

Regarding the slit-film geotextile, the results are mixed. Whether the biaxial loads are applied with the L/T ratio constant or variable, the FOS and permeability decreases (Fourie and Addis 1997). In the 1999 study two types of slit-film woven geotextiles were tested and resulted in conflicting trends. The thicker silt-film sample experiences a decrease in FOS, while the thinner sample has an increase in FOS, with the application of biaxial loads, $L/T = 1$. The thicker sample experiences a decrease in FOS as well, when loaded with a variable L/T ratio. This study's results illustrate an increasing trend in permeability with applied biaxial loads.

6 CONCLUSION

This study explored the effect of tensile biaxial loads on geotextile permittivity and compared the deduced results to uniaxial behavior. It was found that the filtration behavior of the nonwoven geotextiles in the biaxial condition was similar to that of the same nonwoven geotextiles in the uniaxial condition. This was not true, however for more complex weaved woven geotextiles. The applied biaxial tensile loads had a different effect on the deformation of the geotextile fibers and the resulting changes in pore size as compared to the effect of uniaxial tensile loads. This was evidenced by the flow rate behavior of the woven polypropylene geotextiles, whereby a limiting magnitude of increase or decrease in flow rate that was achieved, in the biaxial condition, as indicated by the asymptotic trend of the respective graphs of applied longitudinal load versus flow rate retained. In the case of the slit-film woven geotextile however, the effect of the uniaxial and biaxial tensile loads on filtration were essentially the same.

ACKNOWLEDGEMENTS

The test specimens of this project were provided by the Ocean-Coastal Company. Miss Edwards is supported by the ASEE-GAANN Fellowship.

REFERENCES

- ASTM D 4491. Standard Test Methods for Water Permeability of Geotextiles by Permittivity, *American Society for Testing and Materials*, West Conshohocken, Pennsylvania, USA.
- ASTM D 4885. Standard Test Methods for Permittivity of Geotextiles Under Load, *American Society for Testing and Materials*, West Conshohocken, Pennsylvania, USA.
- ASTM D 5493. Standard Test Methods for Permittivity of Geotextiles Under Load, *American Society for Testing and Materials*, West Conshohocken, Pennsylvania, USA.
- Edwards, M., Hsuan, G., and Kastner, J. 2009. Permittivity of Geotextiles with Uniaxial Tensile Loads, *Geosynthetics 2009*, Salt Lake City, Utah, Feb. 25-27.
- Fourie, A.B. and Addis, P.C. 1999. Changes in filtration opening size of geotextiles subjected to tensile loads, *Geotextiles and Geomembranes* Vol. 17, pp. 331-340.
- Fourie, A.B. and Addis, P.C. 1997. The Effect of In-Plane Loads on the Retention Characteristics of Geotextiles, *Geotechnical Testing Journal*, GTJODJ, Vol. 20(2), pp. 211-217.
- Gaffney, D.A., Hsuan, G., Weggel, J.R., and Munoz, R. 2009. Drainage Characteristic of Geotextiles under Tensile Loads, *Geosynthetics 2009*, Salt Lake City, Utah, Feb. 25-27.